Sensitivity of the Hawt noise level predicted based on Amiet's theory on the value of a turbulence intensity coefficient determined numerically

Katarzyna Suder-Dębska[1,*], *Dawid* Romik[1], and *Ireneusz* Czajka[1]

[1]AGH University of Science and Technology, Department of Power Systems and Environmental Protection Facilities, Mickiewicza 30 Av. 30-065Cracow, Poland

Abstract. In the paper the authors presented and compared two methods of the HAWT noise predicting. The priority, however, was to test the possibility of using Amiet's theory to determine the noise value in the far field. In this theory it is necessary to know the value of the turbulence intensity coefficient. The value of this coefficient was determined based on numerical modeling. The NACA 0012 profile was used for the airfoil shape. The ANSYS/Fluent program was used for numerical calculations, where the k–ω SST turbulence model was used to simulate the flow, and Ffocs-Williams and Hawkings model was used to determine the noise level. The turbulence intensity coefficient estimated in this way was then used to determine the noise value from the wind turbine airfoils using Amiet's theory.

1 Introduction

Sustainability requires that along with technological development providing adequate comfort of life, while at the same time carrying for the natural environment. It seems as close as possible to obtain energy from renewable sources as far as possible. Wind turbines, for example, can be such a solution. Often, however, there are situations in which residents of a given area have a negative feeling in relation to such investments. Their position is based, for example, on the impression of too loud sound generated by wind turbines. Because noise is a subjective impression, the solution to such a situation may be to present the obtained sound pressure level from a given object. For existing objects, these results can be obtained based on measurements in the environment. For designed object seem to be necessary the forecasts obtained, for example, on a numerical way. It is necessary to have full information about the sound source to correctly carry out the numerical simulations. It this paper the authors presented and compared two methods of the HAWT noise predicting. It also presents how the value of the sound level changes depending on the wind parameters.

* Corresponding author: suder@agh.edu.pl

1.1 Research object

For this example a model of a wind turbine consisting of three 45 m long blades was adopted. The chord length is 3.5 m at the root of the blade and 0.8 m at the tip. The blades geometries were chosen so that the angle of attack (AoA) over the entire blade length was 4º. However, according to [1] turbulent inflow noise is almost independent of AoA for symmetric airfoils such as NACA 0012 (described above).

2 Numerical simulation

The Ffowcs Williams Hawkings [2] acoustic model (FW-H) available in the ANSYS/Fluent program was used to determine the sound pressure level of the model rotor. The FW-H model takes the general form of the Lighthill's acoustic analogue [3] and is able to predict the sound generated by equivalent acoustic sources such as monopoles, dipoles and quadrupole. The ANSYS/Fluent program adopts an equation in which the acoustic pressure and acoustic signal at designated points of the receiver is calculated by determining several integrals on the surface. The FW-H equation is a non-homogeneous wave equation that can be determined by the coupling of continuity equations and Navier-Stokes equations. The FW-H equation can be written as:

$$\frac{1}{a_0^2}\cdot\frac{\partial^2 p'}{\partial t^2}-\nabla^2 p' = \frac{\partial^2}{\partial x_i \partial x_j}\left\{T_{ij}H(f)\right\}-\frac{\partial}{\partial x_i}\left\{\left|P_{ij}n_j+\rho u_i\left(u_n-v_n\right)\right|\delta(f)\right\}+ \\ +\frac{\partial}{\partial t}\left\{\left|\rho_0 v_n+\rho\left(u_n-v_n\right)\right|\delta(f)\right\}=0 \tag{1}$$

where :

u_i	–	fluid velocity component in the x_i direction,
u_n	–	fluid velocity component normal to the surface $f = 0$
v_i	–	surface velocity component normal to the surface,
$\delta(f)$	–	Dirac delta function,
$H(f)$	–	Heaviside function,
p'	–	sound pressure at the far field $(p'-p_0)$
n_i	–	unit normal vector pointing toward the exterior region $(f > 0)$,
a_0	–	far-field sound speed,
T_{ij}	–	Lighthill stress tensor,
P_{ij}	–	compressive stress tensor.

The surface $f = 0$ corresponds to the source (emission) surface, and can be made coincident with a body (impermeable) surface or a permeable surface off the body surface.

$$T_{ij}=\rho u_i\left(u_n-v_n\right)+P_{ij}-a_0^2\left(\rho-\rho_0\right)\delta_{ij} \tag{2}$$

$$P_{ij}=p\delta_{ij}-\mu\left[\frac{\partial u_i}{\partial x_j}+\frac{\partial u_j}{\partial x_i}-\frac{2}{3}\frac{\partial u_k}{\partial x_k}\delta_{ij}\right] \tag{3}$$

The solution of equation (1) is obtained using the free-space Green function $\delta(g)/(4\pi r)$. The complete solution consists of surface integrals and volume integrals. The surface integrals represent the contributions from monopole and dipole acoustic sources and partially from quadrupole sources, whereas the volume integrals represent quadrupole (volume) sources in the region outside the source surface. The contribution of the volume integrals becomes small when the flow is low subsonic and the source surface encloses the source region. In ANSYS/Fluent, the volume integrals are dropped. Thus, one has

$$p'=(x,t)=p_T'(x,t)+p_L'(x,t) \tag{4}$$

$$4\pi p_T'(x,t)=\int_{f=0}\left[\frac{\rho_0\left(\dot{U}_n+U_{\dot{n}}\right)}{r\left(1-M_r\right)^2}\right]dS+\int_{f=0}\left[\frac{\rho_0 U_n\left\{r\dot{M}_r+a_0\left(M_r+M^2\right)\right\}}{r^2\left(1-M_r\right)^3}\right]dS \tag{5}$$

$$4\pi p_L'(x,t)=\frac{1}{a_0}\int_{f=0}\left[\frac{\dot{L}_r}{r\left(1-M_r\right)^2}\right]dS+\int_{f=0}\left[\frac{L_r-L_M}{r^2\left(1-M_r\right)^3}\right]dS+\frac{1}{a_0}\int_{f=0}\left[\frac{L_r\left\{r\dot{M}_r+a_0\left(M_r+M^2\right)\right\}}{r^2\left(1-M_r\right)^3}\right]dS \tag{6}$$

where:

$$U_i=v_i+\frac{\rho}{\rho_0}\left(u_n-v_i\right) \tag{7}$$

$$L_i=P_{ij}\hat{n}_j+\rho\,u_i\left(u_n-v_n\right) \tag{8}$$

where :

n, r – unit vectors in the radiation and wall-normal directions,

M – Mach number of a source.

Taking into account the observer time t and the distance to the observer *r*, the integral of the above equation is computed in time defined by the equation :

$$\tau=t+\frac{r}{a_0} \tag{9}$$

2.1 Numerical model

All numerical calculations were done in ANSYS/Fluent. On the rotor blades and the walls of the enclosure, a Wall boundary condition is provided which prevents air from flowing through these surfaces. At the inlet, the boundary condition Velocity inlet U=8 m/s. At the outlet the pressure outlet was determined so that it corresponded to the barometric pressure $p = 0$. The rotational speed of the rotor is 14 rpm and the simulation uses the Sliding Mesh approach. The time step $\Delta t=1\cdot10^{-4}$ s was adopted. The equation of continuity and Navier-Stokes with Reynolds averaging (RANS) were used for the calculations. The two-mode Menter's turbulence model *k–ω* SST was adopted [4][5]. For the above input data, the model quickly reached convergence and the results matched the expected results.

The *k–ω* SST model is a model that combines the advantages of the *k–ε* and *k–ω* model and introduces an additional limiting factor for the over-production of turbulent kinetic energy in the areas of strong positive pressure gradients (accumulation points, separation of the boundary layer regions). By examining the *k–ε* and *k–ω* models, Menter observed that the first one models well the turbulence in free flow and shear layers and is characterized by low sensitivity to inlet conditions for turbulence volumes. This is a desirable feature due to the fact that often in practical calculations these quantities are not exactly known. The *k–ω* model is much better at modeling the turbulent flow in the boundary layer, but it is very sensitive to turbulent values in free flow [4].

As an acoustic model Ffowcs-Williams and Hawkings was adopted. The sound pressure level were measured at 100 m distance from the rotor in rotor axis direction behind the turbine.

As a result of the simulations described above, the average values of turbulence intensity on the blade of approx. 14% (Fig.1) was obtained. Fig.2 shows the turbulence intensity values

obtained along the length of the blade. It is easy to notice that the highest values of turbulence intensity are obtained on the tip of the blade, while the lowest in the root area. Between the root and tip areas, turbulence intensity values are approximately the same, i.e. they show differences of no more than 10 percentage points.

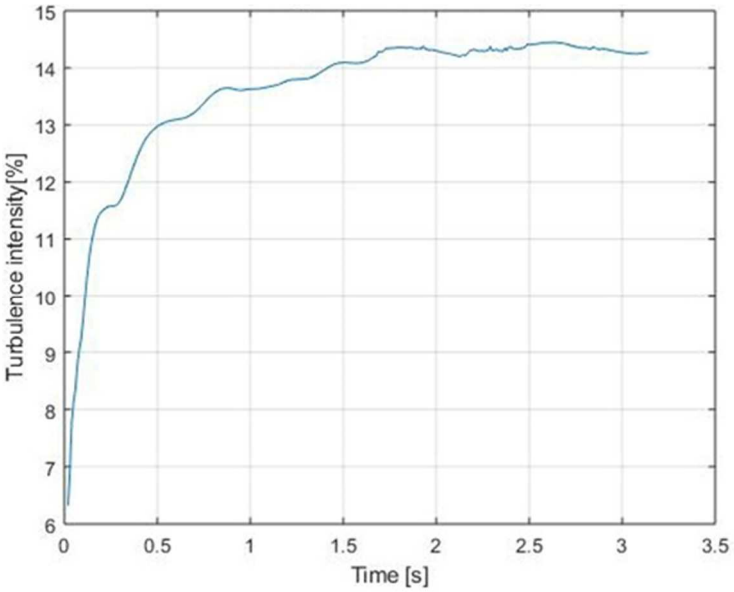

Fig. 1. Average values of turbulence intensity on the airfoil

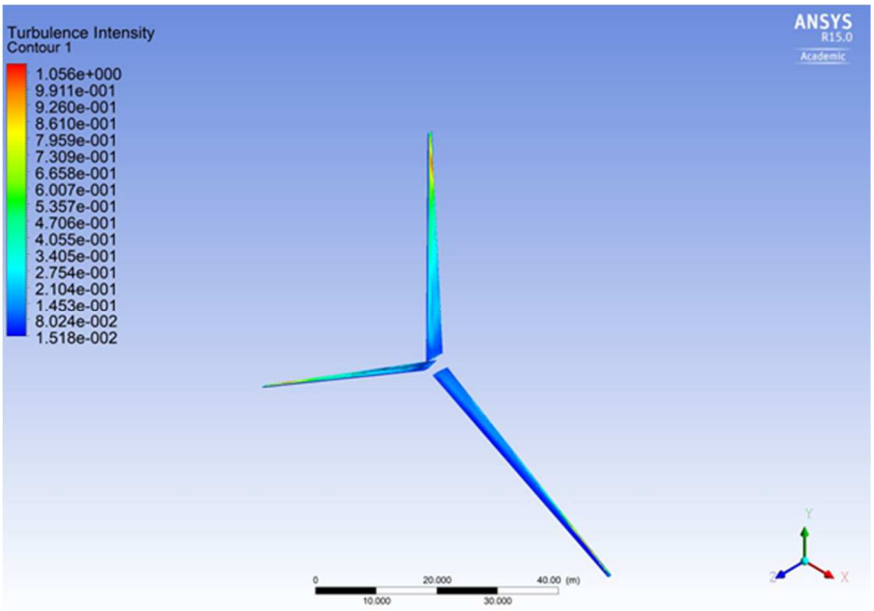

Fig. 2. Values of turbulence intensity along the blade length

3 Main assumptions of Amiet's theory

Amiet's theory concerns the generation of noise through a thin plate under the influence of turbulent flow. The plate is an approximation of the airfoil. The eddies appearing on its surface, pressure fluctuations are treated as dipole sound sources.

In the classic Amiet's theory the airfoil is reduced to a flat plate with zero thickness and a zero angle of attack. The basic assumptions are as follows [6-11]:

- the flow is uniform with velocity U,
- the turbulence fluctuation is small in relation to mean flow velocity,
- the interactions between the airfoil and the turbulent flow can be described as inviscid, so the problem is reduced to the solution of the linearized Euler equation,
- the turbulence is frozen - turbulent gust properties are unchanged while it is convected by the mean flow,
- velocity fluctuation of turbulent gust is represented in terms of chordwise (k_x)and spanwise (k_y) wavenumbers.

In Amiet's theory is used the following equation to calculate the one-third octave sound pressure level (in all parameters, elements related to length are expressed in feet)

$$SPL_{1/3} = 10\log_{10}\left[\frac{L\cdot d/2}{z^2}M^5\frac{\overline{u}^2}{U^2}\frac{\hat{k}_x^3}{\left(1+\hat{k}_x^2\right)^{7/3}}\right]+181.3 \tag{10}$$

where :

L – integral length scale of turbulence,
d – airfoil span,
$\overline{u}^2$ – turbulence intensity,
k_x – chordwise turbulence wavenumber,
$\hat{k}_x = \frac{k_x}{k_e}$,
$k_e = \frac{\sqrt{\pi}}{L}\frac{\Gamma(5/6)}{\Gamma(1/3)}$.

4 Results

Fig.3 presents the results of calculations of the sound pressure level in one-third octave bands for different (changing) values of the intensity coefficient of turbulence obtained by simulation. These values have changed in the range of 6.5-14.5% at one percentage point.

The highest value of turbulence intensity determined on the simulation way was 109%. For this value, the SPL in one-third octave bands generated by the wind turbine was determined at a distance of 100 m from the turbine. Also for this value of the turbulence intensity, the SPL in the one-third octave bands was determined based on the Amiet's theory. The obtained results have been presented in the graph (Fig.4).

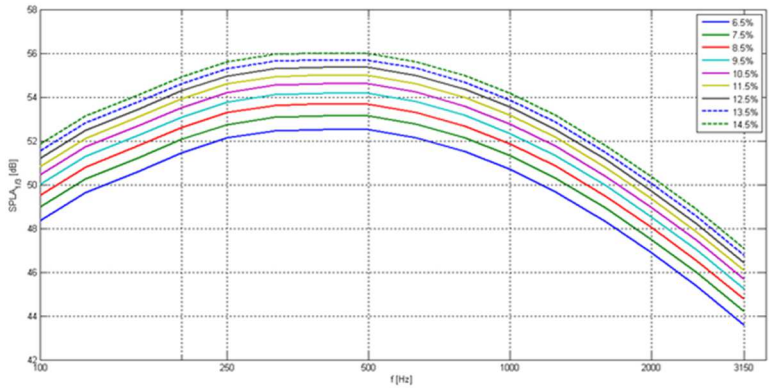

Fig. 3. SPL values depending on the turbulence intensity value

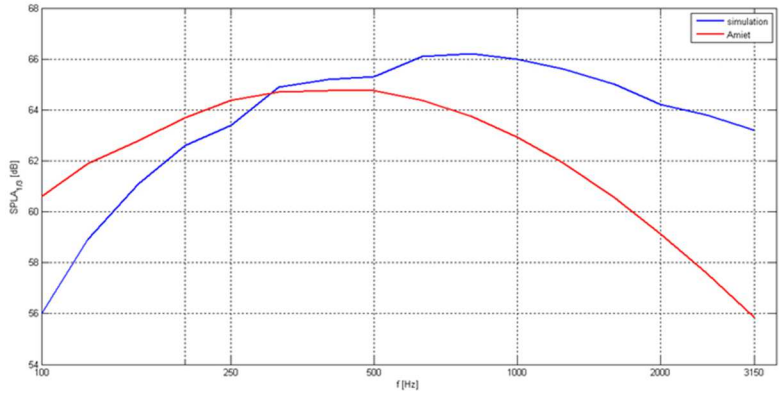

Fig. 4. SPL for turbulence intensity equal to 109% calculated based on simulation and Amiet's theory

The number of numerical experiments were reduced by using DOE. An extended central composite face centered (CCF) design in which factors adopt values on five levels were used. For four factors x_1, x_2, x_3 and x_4 there is a need to conduct 49 numerical experiments. The calculations were performed using "ZEUS" supercomputer at ACK Cyfronet Krakow. The table 3 presents the plan of the conducted simulations with the input and output parameters.

5 Conclusion

The article has presented the considerations on the influence of turbulence intensity values on the obtained SPL. In detail, this impact has been analyzed for the turbulence intensity in the range of 6.5-14.5%. As might be expected, along with the increase of the turbulence intensity, the obtained SPL also grows. For values within the range of up to 10%, a change by one percentage point may lead to a change in SPL values even by 1 dB. For the higher turbulence intensity values, these changes will of course also appear, but they are not so clear.

Since the greater the intensity of turbulence, the higher the SPL values, it can be assumed that for a turbulence intensity of 109%, the obtained SPL value will be the highest possible. Both in simulations and in calculations based on Amiet's theory, the SPLA values in the one-third octave bands at the level of approx. 65 dB were obtained. The SPLA values determined

in both ways show differences in the lowest and highest frequencies analyzed. However, this is still a value of several decibels. The results for frequencies in the range of 200-1000Hz are promising - the differences in obtained values is much less than 3 dB.

Because the obtained SPLA values are similar, one can expect that similar values will also be obtained under real conditions. It seems important to verify the correctness of the obtained values of turbulence intensity, because as one can see it significantly affects the value of the noise generated by wind turbines. Fig

References

1. Devenport W., Staubs J., Glegg S., Sound radiation from real airfoils in turbulence, Journal of Sound and Vibration, **329**, pp. 3470–3483, (2010)
2. Ffowcs-Williams J. E., Hawkings D. L., Sound Generation by Turbulence and Surfaces in Arbitrary Motion, Proc. Roy. Soc., London, pp. A264:321–342, (1969)
3. Lighthill M.J., On Sound Generated Aerodynamically, Proc. Roy. Soc., London, pp. A211:564-587, (1952)
4. Menter F.R., Zonal Two Equation Turbulence Models for Aerodynamic Flows, AAIA Paper, pp. 93-296, (1993)
5. Ansys Fluent.: Theory Guide. Ansys Inc. (2015)
6. Amiet R.K. Acoustic Radiation from an Airfoil in a Turbulent Stream, Journal of Sound and Vibration, **41**, 4, pp. 407-420, (1975)
7. Amiet R. K. Noise due to Turbulent Flow past a Trailing Edge, Journal of Sound and Vibration, **47**, 3, pp. 387-393, (1976)
8. Paterson R.W., Amiet R.K. Acoustic radiation and surface pressure characteristics of an airfoil due to incident turbulence, National Aeronautics and Space Administration: Washington, USA, (1976)
9. Schlinker R.H., Amiet R.K. Helicopter Rotor Trailing Edge Noise, National Aeronautics and Space Administration: Washington, USA, (1981)
10. Roger M., Moreau S. Extensions and Limitations of Analytical Airfoil Broadband Noise Models, International Journal of Aeroacoustics, **9**, 273-305, (2010)
11. Tian Y., Cotte B. Wind Turbine Noise Modeling Based on Amiet's Theory: Effects of Wind Shear and Atmospheric Turbulence, Acta Acustica united with Acustica, **102**, 102, pp. 626-639, (2016)